IEEE Journal of Microwaves

Received 5 October 2020; revised 16 November 2020; accepted 17 November 2020.
Date of current version 7 January 2021.

Digital Object Identifier 10.1109/JMW.2020.3039421

Supply Modulation Behavior of a Doherty Power Amplifier

DAN FISHLER (Member, IEEE), ZOYA POPOVIĆ (Fellow, IEEE), AND TAYLOR BARTON (Senior Member, IEEE)

(Contributed Paper)

University of Colorado Boulder, Boulder, CO 80309 USA

CORRESPONDING AUTHOR: Taylor Barton (e-mail: taylor.w.barton@colorado.edu).

This work was supported by Analog Devices.

ABSTRACT This paper presents a study of supply modulation in a Doherty power amplifier (DPA). To validate a simplified theoretical model, a 3.5 GHz conventional symmetrical DPA using a 6-W packaged GaN pHEMT is designed for supply modulation of the main and/or auxiliary amplifiers. The DPA is characterized in CW operation over a range of supply voltages, and shows up to 15 percentage point efficiency improvement at 12 dB output back-off when both main and auxiliary amplifiers are varied simultaneously. A comparison of three cases of supply variation is shown and potential benefits for improving back-off efficiency are discussed.

INDEX TERMS Doherty PA, gallium nitride (GaN), load modulation, power amplifier (PA), supply modulation.

I. INTRODUCTION

Modern communications systems require high data rates confined within a limited spectrum, resulting in signals with peak-to-average power ratios (PAPRs) exceeding 10 dB. To maintain high efficiency in the power amplifier (PA) under these conditions, multiple efficiency enhancement techniques can be combined. In particular, the efficient output power range of the popular Doherty power amplifier (DPA) [1], [2] can be extended using supply modulation (SM).

Although SM is typically applied to single-ended PAs as overviewed in e.g. [3], it has been successfully demonstrated with other efficiency enhancement techniques including Chireix outphasing [4], load-modulated balanced [5], [6] and Doherty PAs [7]–[11]. Operating the main PA (MPA) and auxiliary PA (APA) in a DPA with different static supply voltages to extend the efficient range is shown in [7]. Dynamically modulating the MPA [8], [9] was shown to increase efficiency in back-off by 15 percentage points [8], while modulating the APA supply was shown to increase efficiency in the high-power regime [10]. Modulating both MPA and APA supplies together increases the back-off efficiency range [11].

This work presents a systematic study of the effect of SM on the behavior and overall performance of the DPA. Three modulation strategies are compared: MPA only; APA only; and both together. A simple theoretical model that captures clipping effects is developed and measurements performed to validate the predicted trends. Previous work in [12] presented characterization under supply modulation of a Doherty-type PA, designed for linearity using the "black box" method [13]. Here we present an extended theoretical analysis for a conventionally-designed DPA under different forms of SM, along with a detailed simulated comparison of the load modulation conditions for each type of SM. Measured performance on a 3.5 GHz DPA with static supply variation shows that the simple model predicts the measurements for the different SM modes.

II. OPERATING PRINCIPLES OF THE SM-DPA

When the MPA supply is reduced, the MPA will clip before the APA turns on, modifying the load modulation. If the APA is supply modulated, the peak output power of the DPA will be limited by the maximum voltage swing of the APA. These behaviors can be captured with a simplified theoretical model. We assume that the current of both PAs depends only on v_{in} and remains below $I_{\max}$, that the APA always turns on at $V_{in,\max}/2$ and that there are no knee effects. The currents in

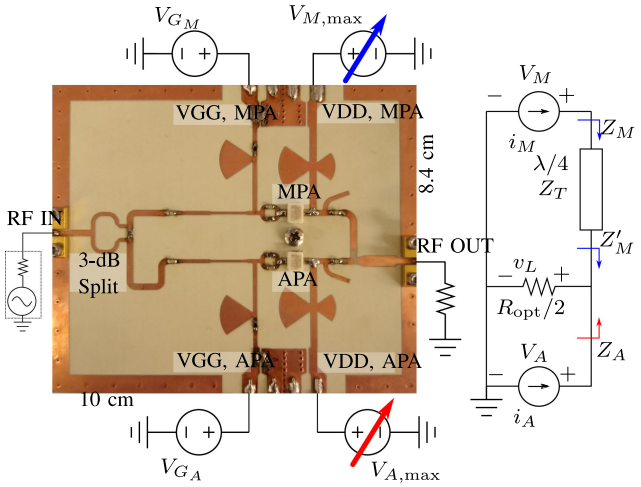

FIGURE 1. Illustration of supply modulation of a DPA used to enhance efficiency, showing the two variable supply voltages: main PA supply V_M and auxiliary PA supply V_A. The symmetric DPA designed at 3.5 GHz is fabricated on a Rogers 4350 substrate with Cree 6-W GaN devices.

the DPA are then independent of supply voltage and identical to standard simplified linear profiles given by [2]:

$$i_M = I_{\max}\left(v_{in}/V_{in,\max}\right),\ 0 < v_{in} < V_{in,\max} \tag{1}$$

$$i_A = \begin{cases} 0, & 0 < v_{in} < \frac{V_{in,\max}}{2} \\ I_{\max}\left(\frac{v_{in}-V_{in,\max}/2}{V_{in,\max}/2}\right), & \frac{V_{in,\max}}{2} < v_{in} < V_{in.\max} \end{cases} \tag{2}$$

When either branch PA undergoes supply modulation, its voltage will clip and that PA will operate as a voltage source instead of as a current source, modifying the DPA operation. The clipping behavior is treated following the analysis in [1] for overdriven class B PAs, i.e. a clipping angle is calculated and from that of the fundamental voltage component.

In the SM-MPA case, the MPA current increases linearly with input drive while the fundamental component of the voltage increases more slowly, leading to variation in the effective load Z_M (graphically defined in Fig. 1) seen at the fundamental frequency. The fundamental component of the MPA output voltage is calculated from an ideal clipping angle in terms of the input drive as in [1], and the result is plotted in Fig. 2(b). We follow the convention in DPA analysis in which the voltage across the APA is calculated based on the node voltages of the network even when that PA is turned off in back-off.

When the APA begins to contribute current, the MPA voltage remains clipped and both amplifiers are load modulated. This effect is seen in Fig. 2, where the case $V_{M,\max} = 0.5V_{A,\max}$ is shown. Note that the DPA output voltage is equal to the voltage across the APA and is calculated from power conservation, based on the quadratic equation $v_L^2/Z_L = v_M i_M + v_L i_A$. Here i_M and i_A are the currents generated by the two amplifiers and v_M is the magnitude of the MPA output voltage. We note that the plotted MPA voltage exceeds a 0.5 normalized value because the MPA saturates. From Fig. 2(c), the load impedances to the MPA and APA at peak power are

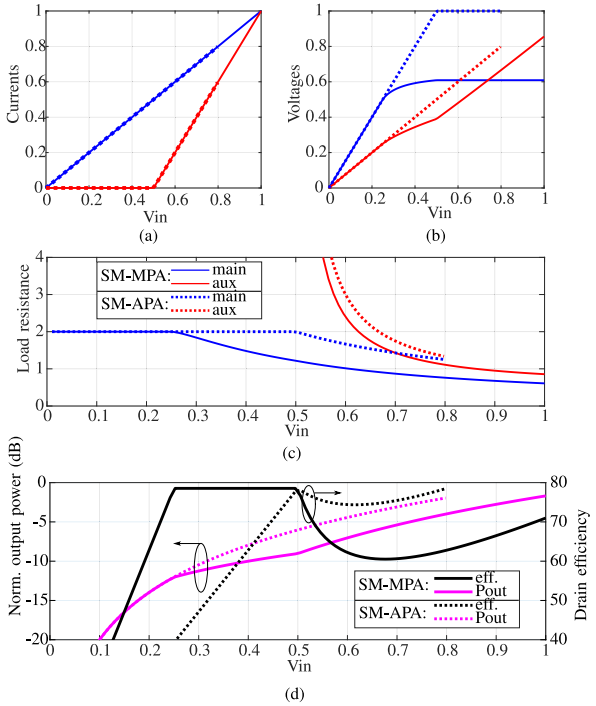

FIGURE 2. Calculated clipping behavior of ideal DPA main and auxiliary devices for the normalized cases $V_{M,\max} = 0.5V_{A,\max}$ (SM-MPA, solid lines), and $V_{A,\max} = 0.8V_{M,\max}$ (SM-APA, dashed lines).

both less than the nominal $R_{\rm opt}$. In addition to modulating the DPA output power, therefore, supply modulation also modifies the range of impedances seen by the branch PAs.

The analysis for APA supply modulation is similar, with output voltage v_L (and therefore output power) limited by the maximum swing of the APA. Fig. 2 shows the DPA operation when the APA is supply modulated such that $V_{A,\max} = 0.8V_{M,\max}$. These example values correspond roughly to the $V_{M,\max} = 28$ V, $V_{A,\max} = 22$ V condition that is validated in the experimental work presented in Section III. It is assumed that the DPA will not be overdriven past clipping due to the gain compression that would occur. The range of load impedances is modified in this case also; the load impedances to the MPA and APA at peak power are now both greater than the nominal $R_{\rm opt}$.

The theoretical drain efficiency versus input voltage is shown in Fig. 2(d) for the SM-MPA and SM-APA cases. These calculations follow the standard DPA approach of assuming both PAs are in ideal class B with (non-clipping) peak efficiency of 78.5% and efficiency proportional to output voltage. It can be seen that reducing the APA supply moves the higher-power efficiency peak to a lower output power level; reducing the MPA supply moves the lower-power efficiency peak; and modulating both supplies together moves both peaks. Because the APA turn-on is fixed at a particular input voltage, cases in which the MPA clips before the APA turns on causes a region of overdriven MPA (shown as flat efficiency) rather than a simple shift in power of both peaks.

This will correspond to a region of reduced gain due to MPA compression.

III. DPA DESIGN AND CHARACTERIZATION

A 3.5-GHz 12-W symmetric DPA with two CREE CGH40006 6 W GaN devices is designed based on manufacturer-provided large-signal models, following the standard DPA approach with a quarter-wavelength inverter in the combiner network and offset lines [2]. Because of the intended use with supply modulation, the drain bias network is designed with radial stubs and no discrete capacitors, while maintaining stability. The MPA and APA have identical bias and stability networks, and are biased in class B and deep C, respectively. The additional phase shift due to the different values of non-linear capacitances C_{DS} and C_{GS} at the different bias conditions is compensated using offset lines in the combiner and a compensation line at the input of the APA [2]. A photograph of the DPA is shown in Fig. 1.

Fig. 3 presents the simulated load trajectories at the intrinsic plane of each PA. Also shown are the simulated load-pull impedance targets at peak output power and at 6-dB output back-off. Three scenarios of variable supply voltages are simulated: 16–28 V variation for both MPA and APA in even increments; variation of MPA supply with APA kept at its nominal $V_A = 28$ V; and variation of APA supply with MPA kept at its nominal $V_M = 28$ V. In addition to the standard power-dependent DPA load modulation, variation in load trajectories is observed when the supply varies.

In a supply modulation application, when only the MPA supply is modulated we expect that both the MPA and APA see lower-impedance loads at peak output power, as is indeed observed from Fig. 3. When only the APA is supply modulated, both loads trend towards higher impedances. When both supplies are modulated, the loads at peak output power converge to the nominal case, although nonlinear effects cause a spreading in the contours at mid-power levels. The qualitative behavior agrees with what is expected from the simplified theory (Fig. 2), but with added reactive variation due to AM-PM effects in the MPA and APA.

The DPA is characterized in CW operation and static supply voltage variation, with results summarized in Fig. 4. In this figure, each measured or simulated curve shows a single CW drive-up characterization at a particular constant supply voltage. As in the simulations shown in Fig. 3, the swept supply voltages range from 16 to 28 V in 2-V steps. Overall, the measured and simulated characteristics across the three SM cases have similar shapes, although the back-off efficiency peak occurs at around a 2-dB higher power than predicted. This discrepancy is attributed to the large-signal operation in a class-C bias and supply modulation—neither condition for which the large-signal model is optimized. A slight degradation in measured gain matches our past experience using the same model. It is observed that SM of both PAs or SM of the MPA alone while keeping the APA in nominal bias is most beneficial. SM of both PAs yields a 0–5 percentage points higher efficiency in the high-power region, while the gain performance of the two cases are nearly identical. However, SM of the MPA alone might be more practical, both in terms of complexity and timing considerations, for example, to avoid added interconnect inductance [12].

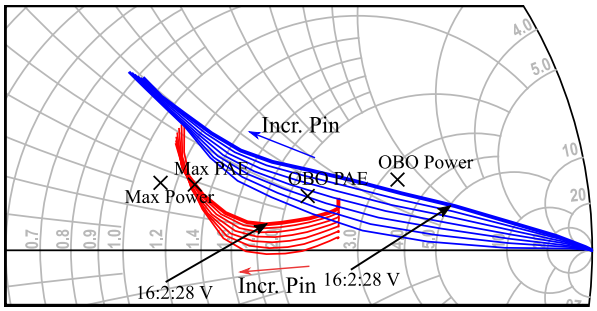

(a) SM both

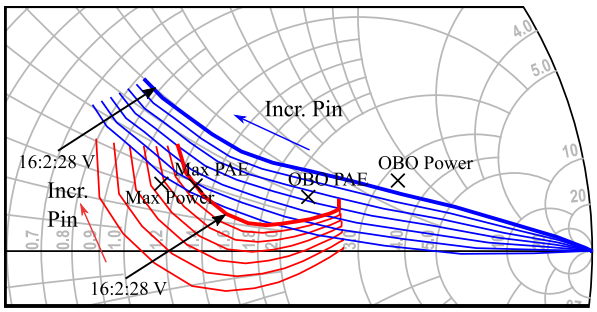

(b) SM MPA, APA supply 28 V

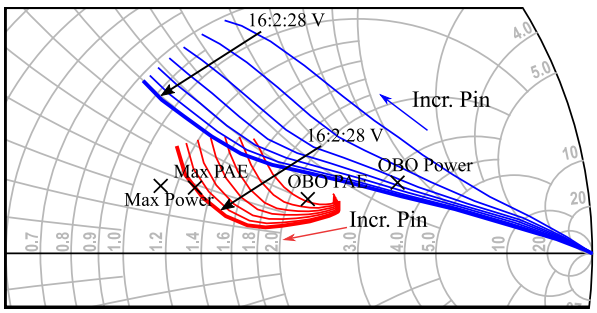

(c) SM APA, MPA supply 28 V

FIGURE 3. Load modulation trajectories at the intrinsic drain of the MPA (red) and APA (blue) for a power sweep and drain voltages varied from 16–28 V in 2 V increments. The power and efficiency impedance targets from load-pull simulations are shown. Thick lines highlight the nominal 28 V on both drains.

The four different SM strategies are compared to the theoretical analysis in Fig. 5, showing that the simplified theoretical model predicts the behavior of a DPA under different SM scenarios. It is notable that the measured efficiency peak at back-off is less pronounced than expected from theory; this is typical of practical DPAs and is related to the parallel losses of the non-ideal device.

Table 1 compares the measured results with state-of-the-art PAs employing gate and/or supply modulation. The PA in this work demonstrates the highest overall PAE at maximum

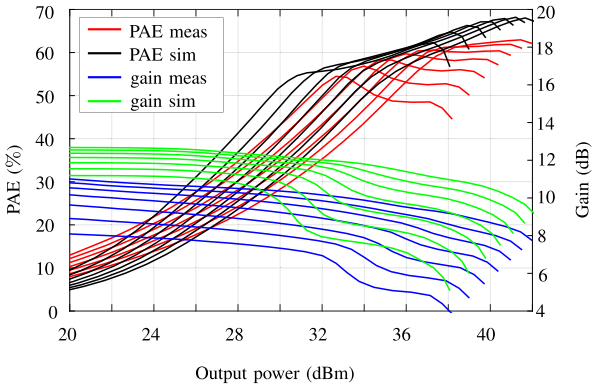

(a) SM both

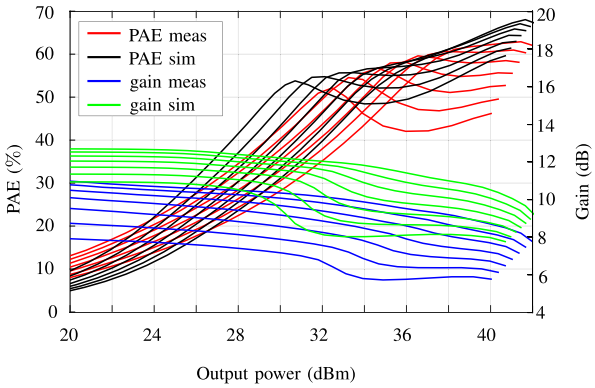

(b) SM MPA, APA supply 28 V

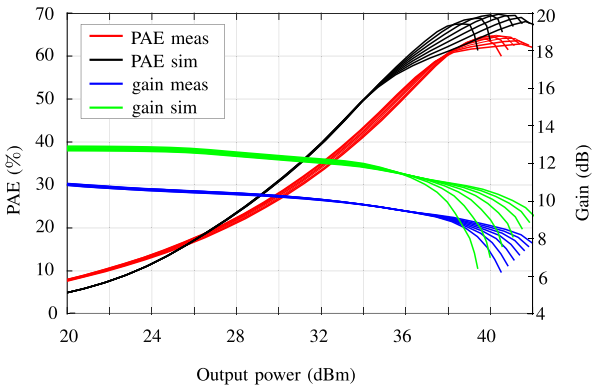

(c) SM APA, MPA supply 28 V

FIGURE 4. Comparison of simulated (black – PAE, green – gain) vs. measured (red – PAE, blue – gain) results for the DPA under various SM schemes.

TABLE 1. DPA Comparison With Gate Modulation (GM) and SM

Ref.	DPA Control Strategy	Freq. (GHz)	P_{out} (dBm)	PAE (%) (0-6-10 dB BO)
[8]	SM MAIN	2.14	43	69 - 58 - 49
[14]	GM MAIN + AUX	2.14	39	49 - 37 - 29
[10]	SM AUX	2.40	44	76 - 63 - 45* (DE)
[15]	GM AUX	2.14	46	47 - 32 - 23
This work	SM MAIN + AUX	3.50	41.6	63 - 60 - 53
	SM MAIN	3.50	41.6	63 - 58 - 51

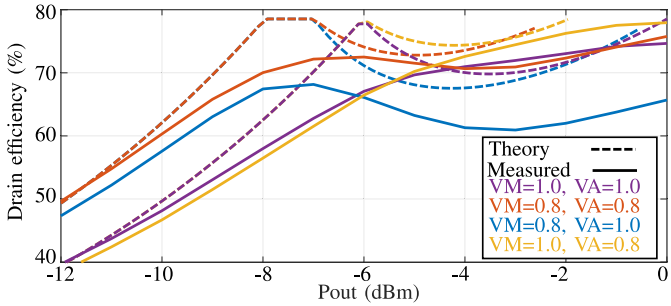

FIGURE 5. Calculated (solid) and measured (dashed) drain efficiency vs. normalized output power of the idealized DPA for multiple normalized supply modulation cases: (1) $V_{M,max} = V_{A,max} = 1$, (2) $V_{M,max} = V_{A,max} = 0.8$, (3) $V_{M,max} = 1$, $V_{A,max} = 0.8$, and (4) $V_{M,max} = 0.8$, $V_{A,max} = 1$. Measured results are normalized to $V_{max} = 28$ V with $0.8V_{max} = 22$ V.

output power and at 10 dB output back-off while operating at the highest frequency.

IV. CONCLUSION

This work compares the benefits of supply modulation within a DPA when the main and auxiliary PAs are modulated independently and together. The standard DPA analysis is adapted to include clipping effects in the MPA and/or APA, predicting variation in the load trajectories due to different static supply voltage conditions. Significant improvement in efficiency at back-off powers up to 10 dB are demonstrated. The nonlinear simulations and measurements presented here are done with static variations of the supply voltages and under CW drive, and the simplified theory is validated. While we expect modified behavior under dynamic supply modulation, the presented approach is a good starting point for SM DPA design and gives insight into the dependence on variable parameters. Although SM of both PAs simultaneously is shown to offer slightly higher efficiency benefits, SM of the MPA alone may be preferable due to its comparable performance and practical simplicity.

REFERENCES

[1] S. C. Cripps, *RF Power Amplifiers for Wireless Communications*, 2nd ed. Norwood, MA, USA: Artech House, 2006.

[2] B. Kim, *Doherty Power Amplifiers from Fundamentals to Advanced Design Methods*. New York, NY, USA: Academic, 2018.

[3] P. Asbeck and Z. Popovic, "ET comes of age: Envelope tracking for higher-efficiency power amplifiers," *IEEE Microw. Mag.*, vol. 17, no. 3, pp. 16–25, Mar. 2016.

[4] T. Cappello, T. W. Barton, C. Florian, M. Litchfield, and Z. Popovic, "Multilevel supply-modulated Chireix outphasing with continuous input modulation," *IEEE Trans. Microw. Theory Techn.*, vol. 65, no. 12, pp. 5231–5243, Dec. 2017.

[5] D. J. Shepphard, J. Powell, and S. C. Cripps, "A broadband reconfigurable load modulated balanced amplifier (LMBA)," in *Proc. IEEE MTT-S Int. Microw. Symp.*, 2017, pp. 947–949.

[6] T. Cappello, P. Pednekar, C. Florian, S. Cripps, Z. Popovic, and T. W. Barton, "Supply- and load-modulated balanced amplifier for efficient broadband 5G base stations," *IEEE Trans. Microw. Theory Techn.*, vol. 67, no. 7, pp. 3122–3133, Jul. 2019.

[7] T. Kitahara, T. Yamamoto, and S. Hiura, "Doherty power amplifier with asymmetrical drain voltages for enhanced efficiency at 8 dB backed-off output power," in *Proc. IEEE MTT-S Int. Microw. Symp.*, Jun. 2011, pp. 1–4.

[8] J. Moon *et al.*, "Doherty amplifier with envelope tracking for high efficiency," in *Proc. IEEE MTT-S Int. Microw. Symp.*, May 2010, pp. 1086–1089.
[9] J. Choi, D. Kang, D. Kim, and B. Kim, "Optimized envelope tracking operation of Doherty power amplifier for high efficiency over an extended dynamic range," *IEEE Trans. Microw. Theory Techn.*, vol. 57, no. 6, pp. 1508–1515, Jun. 2009.
[10] A. Alt and J. Lees, "Improving efficiency, linearity and linearisability of an asymmetric Doherty power amplifier by modulating the peaking amplifier's supply voltage," in *Proc. Eur. Microw. Conf.*, Oct. 2017, pp. 464–467.
[11] Y. Park, J. Lee, S. Kim, D. Minn, and B. Kim, "Analysis of average power tracking Doherty power amplifier," *IEEE Microw. Wireless Compon. Lett.*, vol. 25, no. 7, pp. 481–483, Jul. 2015.
[12] D. Fishler, T. Cappello, W. Hallberg, T. W. Barton, and Z. Popovic, "Supply modulation of a linear Doherty power amplifier," in *Proc. 48th Eur. Microw. Conf.*, pp. 519–522, Sept. 2018.
[13] W. Hallberg, M. Özen, D. Gustafsson, K. Buisman, and C. Fager, "A Doherty power amplifier design method for improved efficiency and linearity," *IEEE Trans. Microw. Theory Techn.*, vol. 64, no. 12, pp. 4491–4504, Dec. 2016.
[14] J. Cha, Y. Yang, B. Shin, and B. Kim, "An adaptive bias controlled power amplifier with a load-modulated combining scheme for high efficiency and linearity," in *IEEE MTT-S Int. Microw. Symp. Dig.*, Philadelphia, PA, USA, vol. 1, Jun. 2003, pp. 81–84.
[15] Z. Zhang and Z. Xin, "A LTE Doherty power amplifier using envelope tracking technique," in *Proc. Int. Conf. Electron. Packag. Technol.*, Aug. 2014, pp. 1331–1334.

DAN FISHLER (Member, IEEE) was born in Tel-Aviv, Israel and received the B.Sc. degree in electrical engineering with minors in mathematics and physics (*magna cum laude*) from Tennessee State University in 2016. Prior to joining the RF Group, he was with the University of Colorado, Boulder, where he received the M.Sc. degree in electrical engineering in 2020. He was with the Industry Designing Control Systems and Image Acquisition Systems for SolVIS, Inc. He is currently with Maxentric, San Diego. His research interests include high-efficiency and high-power microwave amplifiers and related measurements.

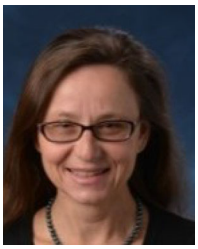

ZOYA POPOVIĆ (Fellow, IEEE) received the Dipl.Ing. from the University of Belgrade, Belgrade, Serbia, and the Ph.D. degree from Caltech, Pasadena, California. She is a Distinguished Professor and the Lockheed Martin Endowed Chair with Electrical Engineering, the University of Colorado, Boulder. She was a Visiting Professor with the Technical University of Munich from 2001to 2003, ISAE in Toulouse, France in 2014, and a Chair of Excellence with Carlos III University, Madrid, Spain, from 2018 to 2019. She has graduated over 60 Ph.D students and currently advises 14 doctoral students. Her research interests include high-efficiency power amplifiers and transmitters, microwave and millimeter-wave high-performance circuits for communications and radar, medical applications of microwaves, and wireless powering. She was the recipient of two IEEE MTT Microwave Prizes for best journal papers, the White House NSF Presidential Faculty Fellow award, the URSI Issac Koga Gold Medal, the ASEE/HP Terman Medal, and the German Humboldt Research Award. She was elected as the Foreign Member of the Serbian Academy of Sciences and Arts in 2006. She was named IEEE MTT Distinguished Educator in 2013 and the University of Colorado Distinguished Research Lecturer in 2015.

TAYLOR BARTON (Senior Member, IEEE) received the SC.B. degree in electrical engineering from the Massachusetts Institute of Technology (MIT), Cambridge, MA, USA in 2006, the M.Eng. degree in electrical engineering, EE degree, and the Sc.D. degree in electrical engineering from MIT in 2006, 2008, 2010, and 2012. She is currently an Assistant Professor with the University of Colorado Boulder, Boulder, CO, USA. From 2014 to 2016, she was an Assistant Professor with the University of Texas, Dallas, TX, USA during which time she was also a Summer Faculty Fellow with the Air Force Research Laboratory, Dayton, OH, USA. In addition to a total of over 70 refereed papers in IEEE technical conferences and journals, she contributed a chapter, "Outphasing Power Amplifiers," to the book *Radio Frequency and Microwave Power Amplfiers*, Volume 2 (IET, 2019). Her research interests include the area of RF and analog circuit design, with focus on energy-efficient RF power amplifiers. Prof. Barton was the recipient of the AFOSR YIP and NSF CAREER Awards.